Geochemical assessment of the palaeoecology, ontogeny, morphotypic variability and palaeoceanographic utility of "Dentoglobigerina" venezuelana

Stewart, Joseph A.; Wilson, Paul A.; Edgar, Kirsty M.; Anand, Pallavi; James, Rachael H.

DOI:
10.1016/j.marmicro.2011.11.003

Geochemical assessment of the palaeoecology, ontogeny, morphotypic variability and palaeoceanographic utility of *"Dentoglobigerina" venezuelana*

Joseph A. Stewart [a,*], Paul A .Wilson [a], Kirsty M. Edgar [a,†], Pallavi Anand [b], Rachael H. James [a]

[a] National Oceanography Centre, Southampton, University of Southampton. SO14 3ZH, UK.
[†] Now at: School of Earth and Ocean Sciences, Cardiff University, Main Building, Park Place, Cardiff, CF10 3AT, UK
[b] Department of Earth and Environmental Science, Walton Hall, The Open University, Milton Keynes, MK7 6AA, UK
*Corresponding author. Tel: +442380599374, Email: Joseph.Stewart@noc.soton.ac.uk

1. Introduction

There is a pressing need to improve our understanding of Oligo-Miocene (O/M) climate change and, in particular, the major perturbation of Cenozoic climate that occurred near the O/M boundary at around 23 Ma (Figure 1). This climate shift is marked by a large increase in the benthic foraminifera $\delta^{18}O$ record (>1.5‰), classically termed the "Mi-1 event" (after the "Mi-1 zone" of Miller et al., 1991), that is now well dated cyclo- and magnotostratigraphically to "$58_{Ol\text{-}C6Cn}$" in the scheme of Wade and Pälike, (2004) and Pälike et al., (2006b). The increase in benthic $\delta^{18}O$ is interpreted to represent major ice sheet expansion on Antarctica (Zachos et al., 2001) associated with a contemporaneous change in the carbon cycle as indicated by an increase in $\delta^{13}C$ of benthic foraminifera (Figure 1).

While benthic foraminiferal $\delta^{18}O$ records provide insight into the timing and magnitude of glaciation, the causes and consequences of the Mi-1 event remain poorly understood. An increase in the ratio of organic carbon to carbonate burial has been invoked (Paul et al., 2000) to account for the $\delta^{13}C$ maximum shown in Figure 1, however, there is little evidence of organic carbon-rich deposits of appropriate age (Lear et al., 2004). Changes in global silicate weathering have a profound effect on the global carbon cycle and climate change on multi-million year timescales (Berner, 1991; Raymo and Ruddiman, 1992; Walker et al., 1981), but relatively little is known about the links between short-term ($<10^5$ yrs) climatic aberrations and silicate weathering (Vance et al., 2009). Nevertheless, variations in chemical weathering rates (and therefore levels of atmospheric carbon dioxide), related to the degree of silicate rock exposure on Antarctica, are hypothesised to account for temperature anomalies observed across the O/M boundary (Lear et al., 2004; *cf.* Kump et al., 1999). A detailed assessment of silicate weathering across the O/M interval is therefore needed to help assess linkages between climate change and this major geological sink for atmospheric CO_2.

Silicate weathering is known to exert a control on the oceanic concentration and isotopic composition of many elements including Li, Os and Nd (Burton and Vance, 2000; Frank, 2002; Huh et al., 2001; Kisakürek et al., 2005; Ravizza and Peucker-Ehrenbrink, 2003).

Arguably the most useful archive for reconstructing the palaeoceanographic record of silicate weathering through use of these elements is planktic foraminiferal calcite recovered from deep-sea sediment cores as exemplified by the pioneering work of Hathorne and James, (2006), Vance and Burton, (1999) and Burton et al., (2010). Unfortunately, all of these elements occur in extremely low abundance within foraminiferal calcite, hence the mass of carbonate required for isotopic analysis is so large (e.g., Nd ~30 mg; Vance and Burton, 1999) that these proxies cannot readily be applied using typical sample suites. One strategy to circumvent this problem is to target particularly large, abundant, long-ranging and cosmopolitan taxa. Such species are rare, but one clear candidate is *"D." venezuelana*, a species that ranges from the early Oligocene to early Pliocene (Bolli and Saunders, 1989; Kennett and Srinivasan, 1983; Olsson et al., 2006; Stainforth et al., 1975), typically possesses medium to large tests (usually 355-400 μm; Spezzaferri, 1994), has a wide geographical distribution (equator to ~50° latitude; Spezzaferri, 1994) and is found in high abundance in tropical O/M sections (Chaisson and Leckie, 1993; Leckie et al., 1993; Pearson and Chaisson, 1997; Spezzaferri, 1994). Yet considerable taxonomic and ecological uncertainties are associated with *"D." venezuelana* and these must be addressed before this taxon can be used for palaeoceanographic purposes with any degree of confidence.

The brief taxonomic description of the holotype specimen (Hedberg, 1937) has led to inclusion of multiple morphotypes under *"D." venezuelana* (Kennett and Srinivasan, 1983; Li et al., 2002; Spezzaferri, 1994; Stainforth et al., 1975), the geochemical validity of which has never been systematically explored. In addition, the depth ecology of *"D." venezuelana* is extremely unclear (Figure 2). Most stable isotope studies of planktic foraminifera assign *"D." venezuelana* to a sub-thermocline habitat (Barrera et al., 1985; Hodell and Vayavananda, 1993; Keller, 1985; Norris et al., 1993; Pearson et al., 2001; Pearson and Shackleton, 1995; Smart and Thomas, 2006; Spezzaferri and Pearson, 2009). However, data generated on samples of O/M boundary age (~23 Ma), from Ceara Rise and Trinidad, imply that *"D." venezuelana* calcified higher in the water column, within the thermocline (Biolzi, 1983; Pearson et al., 1997; Pearson and Wade, 2009). Furthermore, results from analysis of Oligocene (~28 Ma) age samples from the Gulf of Mexico (Poore and Matthews, 1984) and the equatorial Pacific at ODP Site 1218 (Wade et al., 2007), imply that calcification took place within the mixed layer. Establishing the depth habitat of calcification for *"D." venezuelana* across the O/M boundary is a prerequisite for the generation of proxy records of silicate weathering because the concentration of neodymium, and its isotopic composition, vary with depth in the water column (Jeandel, 1993). Similarly, the Li/Ca of planktic

foraminifera may be partly dependent on parameters that change with depth in seawater, such as carbonate ion saturation state (Hall and Chan, 2004).

Here, we present new $\delta^{18}O$, $\delta^{13}C$ and Mg/Ca data from planktic foraminiferal assemblages at ODP Site 925 (Ceara Rise, equatorial Atlantic Ocean) (Figure 2) of O/M boundary age. We determine the effect of test size on $\delta^{18}O$, $\delta^{13}C$ and Mg/Ca, and use these data to explore the ontogenetic variation in the depth habitat of *"D." venezuelana*. We apply a narrow taxonomic concept to *"D." venezuelana*, by identifying three distinct morphotypes. The depth habitat of these morphotypes is inferred from $\delta^{18}O$ and $\delta^{13}C$ analyses, and the geochemical variation within and between morphotypes is established to assess the validity of pooling these intra-specific groups for the purpose of generating "sample hungry" palaeoceanographic records of silicate weathering (e.g., Nd & Li isotopes).

2. Materials and Methods

2.1. Geological setting & chronology

Four samples (see Table 1), spanning the O/M boundary, were analysed from core sediments recovered from ODP Leg 154, Site 925, Hole A (4°12.249'N, 43°29.334'W, 3042.2 m present water depth; Shipboard Scientific Party, 1995a). Magnetostratigraphic age control is not available in ODP Leg 154 sediments, but a high quality magnetostratigraphy is available for ODP Site 1090, Agulhas Ridge (Billups et al., 2002; Channell et al., 2003) and it is correlated to ODP Site 926 (Liebrand et al., 2011), a close neighbour to our study site (ODP Site 925). We tie the ODP Site 925 depth scale to that of ODP Site 926 by peak-matching shipboard magnetic susceptibility and colour reflectance data from both sites. Depth correlation is aided by astronomically matched tie points on either side of the O/M boundary (work of Crowhurst and Shackleton; S. Crowhurst personal written communication[1], 2010) and two biostratigraphic tie points, the first occurrence of *Paragloborotalia kugleri* and the last occurrence of *Sphenolithus delphix* (Pearson and Chaisson, 1997; Shipboard Scientific Party, 1995a; Shipboard Scientific Party, 1995b; Weedon et al., 1997). Sample ages are reported relative to the astronomically tuned age model of ODP Site 926 (Pälike et al., 2006a).

2.2. Taxonomy & morphotypes

In some taxonomic descriptions, the final chamber of *"D." venezuelana* is described as flat, and often small and irregular relative to the penultimate chamber (Spezzaferri, 1994; Stainforth et al., 1975), whereas in other cases chambers in the final whorl are described as increasing regularly in size including specimens with a more inflated final chamber and lobulate test outline (Kennett and Srinivasan, 1983; Li et al., 2002). *"D." venezuelana* has a

relatively narrow umbilical aperture compared to other *Dentoglobigerina* species such as *D. altispira* and *D. globosa*, however, discrepancies also exist in the description of this primary aperture. One study describes the aperture as broadly rectangular or "letter-box" in shape (Kennett and Srinivasan, 1983). A more recent description by Spezzaferri (1994), however, suggests a low-arched aperture in *"D." venezuelana*. Disparity among descriptions of the aperture style likely stem from the low arched aperture seen in the holotype specimen (Hedberg, 1937) and its non-inclusion in the holotype description. The presence of rare supplementary apertures is noted in the holotype description (Hedberg, 1937), however, we find no examples of this species possessing supplementary apertures within our samples. Umbilical teeth are present on the (pen)ultimate chamber(s) of this taxon (see Plate 1), but are variable in size, and can be broken and/or obscured by sediment infilling of the aperture. Hence we do not recommend over-reliance on the presence or absence of umbilical teeth as a defining morphological characteristic when picking specimens for generating palaeoceanographic records.

To help shed light on these taxonomic issues and to assess the geochemical relevance of the variable morphological concepts, we separate *"D." venezuelana* into three distinct morphotypes: 1, specimens with a kummerform, flattened, final chamber and rectangular aperture (Plate 1.1a-f); 2, individuals possessing kummerform, flattened, final chambers and low arched (often asymmetrical) apertures (Plate 1.2a-f); and 3, specimens with a large, embracing final chamber and rectangular aperture (Plate 1.3a-f). In some specimens of morphotype 2 it is difficult to distinguish the cantilevered final chamber from a bulla (for example Plate 1.2a). Every effort is made to verify that these are true final chambers through high magnification examination of the aperture and chamber arrangement in all views, however, in the absence of a final chamber tooth (for example Plate 1.2d), it is almost impossible to definitively show this is not a bulla. All morphotypes have tests with a broadly circular profile, low trochospire and four ovate chambers in the final whorl. All specimens possess the coarse cancellate wall texture characteristic of *"D." venezuelana*.

2.3. Sample preparation

Samples were dried in an oven at 50°C, then gently disaggregated in deionised water using a shaker table and washed over a 63 μm sieve. Single species of foraminifera were then picked from multiple size fractions (212-250, 250-300, 300-355, 355-400, 400-450, 450-500 μm) to obtain 1.2 mg of test calcite per size fraction for each species. Specifically, the three morphotypes of *"D." venezuelana* were picked along with *Catapsydrax ciperoensis, Catapsydrax dissimilis, Catapsydrax indianus, Globigerinoides altiaperturus, Globigerina*

bulloides, "Globigerinoides" primordius, Paragloborotalia bella, and *Paragloborotalia siakensis/mayeri* (Plate 2). Two species of benthic foraminifera, *Cibicidoides mundulus* and *Oridorsalis umbonatus* were also picked for comparison with planktic foraminifera. All tests within each species, single size fraction separate were gently broken open between two glass slides under the light microscope, homogenised and then split. Approximately 200 μg of each sample was used for stable isotope analysis. Where enough material was available, 1 mg of mono-specific broken-open test calcite was analysed for Mg/Ca.

2.4. Stable isotope analysis

Samples were ultrasonicated in deionised water to remove clays and other adhering particles before analysis of stable carbon and oxygen isotopes by a gas source mass spectrometer (Europa GEO 20-20) equipped with an automatic carbonate preparation system (CAPS). Results are presented in the delta notation in ‰ relative to Vienna Pee Dee Belemnite (VPDB). Replicate analyses of an in-house standard are calibrated to NBS-19 and yield a routine external reproducibility of 0.065‰ for $\delta^{18}O$ and 0.031‰ $\delta^{13}C$.

2.5. Mg/Ca analysis

Adhering clay particles were removed through ultrasonication in deionised water and methanol. Samples were then subject to first reductive then oxidative cleaning to remove ferromanganese oxide coatings and organic matter, respectively. Finally, the calcite tests were subjected to a weak acid "polish" to remove any re-absorbed ions (Boyle and Keigwin, 1985; Hathorne, 2004; Rosenthal et al., 1997; Rosenthal et al., 1999).

Foraminiferal calcite was dissolved in 500 μl of 0.075 M HNO_3. An aliquot of this solution was diluted to give a concentration of approximately 3 ppm Ca. Samples were then analysed for Mg and Ca concentrations using a Perkin-Elmer Optima 4300 DV inductively coupled plasma – optical emission spectrometer (ICP-OES). The internal reproducibility of the Mg/Ca ratios, determined by 10 replicate analyses of five multi-element solutions, is <0.21% (1σ; Greaves et al., 2008; Green et al., 2003).

3. Results

3.1. Inter-species stable isotope composition

In Figure 3, we plot $\delta^{18}O$ and $\delta^{13}C$ for benthic and planktic foraminifera from each of our four study samples (Panels I through IV). The sizes of the data points are schematically representative of the size fraction of tests analysed. The planktic foraminifera fall into three distinct groups, (i) *G. bulloides, "G." primordius*, and *G. altiaperturus*, have low $\delta^{18}O$ (~ -2‰) and high $\delta^{13}C$ (~ +2.5‰), (ii) *C. dissimilis, C. ciperoensis*, and *C. indianus* form a group

with high $\delta^{18}O$ (~ +1‰) and low $\delta^{13}C$ values (~ +1‰), and (iii) *P. bella, P. siakensis/mayeri*, and *"D." venezuelana* (morphotype 1) display intermediate $\delta^{18}O$ and $\delta^{13}C$ values. Benthic foraminifera yield the highest $\delta^{18}O$ and lowest $\delta^{13}C$ values of all. $\delta^{13}C$ in *O. umbonatus* is consistently ~1.5‰ lower than in *C. mundulus*. $\delta^{18}O$ in *G. bulloides* (a surface dweller in the modern ocean) is 3.48 to 3.24‰ lower than the $\delta^{18}O$ of *O. umbonatus*. The $\delta^{18}O$ and $\delta^{13}C$ values within each *"D." venezuelana* morphotype vary by up to 0.9‰ and 0.5‰ respectively. Data for the three morphotypes plot within the same isotopic range as one another both before (Figure 3 I′) and after (Figure 3 IV′) the Mi-1 event (Figure 1).

3.2. $\delta^{18}O$, $\delta^{13}C$, and Mg/Ca variation with test size

Figure 4 shows that, in general, in all three morphotypes of *"D." venezuelana*, $\delta^{18}O$ increases with increasing test size in sample I (Figure 4b). $\delta^{18}O$ values show no further increase above the 355-400 μm size fraction. Mg/Ca data for sample I show a trend similar to that seen in $\delta^{18}O$ with values decreasing by >0.5 mmol/mol across the size fraction range measured (Figure 4d). A different distribution, however, is observed in $\delta^{18}O$ and Mg/Ca with test size in sample IV (Compare Figures 4a and c with 4b and d) where variation in $\delta^{18}O$ and Mg/Ca of *"D." venezuelana* within a single size fraction is greater and no obvious trend in $\delta^{18}O$ or Mg/Ca is seen with test size. $\delta^{13}C$ values are tightly grouped within individual size fractions of all *"D." venezuelana* morphotypes analysed both in sample I and sample IV (Figure 4e & f). In both samples, $\delta^{13}C$ increases with increasing test size by approximately 0.5‰ between 212 and 500 μm.

4. Discussion

4.1. Inter and intra-specific calcification depths

$\delta^{13}C$ in foraminiferal test calcite is dependent on the isotopic signature of dissolved inorganic carbon (DIC) in seawater. DIC is removed from seawater during primary production, and ^{12}C is removed in preference to ^{13}C. For this reason, the DIC in surface seawater is isotopically "heavy", whereas deep waters are isotopically "light" because of remineralisation of ^{12}C-enriched organic material (Kroopnick, 1985). Foraminiferal $\delta^{13}C$ is affected by this and a number of other processes that change as a function of depth, such as the photosynthetic activity of symbionts, and irradiance levels (Spero and Williams, 1988; 1989).

The oxygen isotopic composition of ambient seawater ($\delta^{18}O_{sw}$; controlled by ice volume and salinity), and temperature of calcification are the primary controls on the $\delta^{18}O$ of foraminiferal calcite ($\delta^{18}O_c$). Within individual samples at a given location in the ocean, the most important effect on $\delta^{18}O_c$ is temperature; calcification at lower temperatures producing

higher $\delta^{18}O_c$ (Emiliani, 1955). The thermal gradient of the water column in tropical regions means that $\delta^{18}O_c$ can change by as much as 4‰ between species that reside in the mixed layer and species that live deeper in the water column (Biolzi, 1983). Temperature changes most rapidly with depth through the thermocline, therefore, planktic foraminifera calcifying within the thermocline should record a greater change in $\delta^{18}O$ than in $\delta^{13}C$ with increasing depth (Pearson et al., 1993).

In this way, foraminiferal $\delta^{18}O$ and $\delta^{13}C$ can be used to assess the depth habitat of different species and morphotypes from our four samples (Figure 3 I to IV). The $\delta^{18}O$ and $\delta^{13}C$ values of benthic foraminifera are used to constrain temperature and $\delta^{13}C$ in deep waters at this site, respectively. $\delta^{13}C$ is lower in *O. umbonatus* than in *C. mundulus*, consistent with the view that *O. umbonatus*, in general, occupies a shallow infaunal niche below the sediment-water interface, whereas *C. mundulus* calcifies epifaunally (Rathburn and Corliss, 1994). Our stable isotope data for planktic foraminifera shown in Figure 3 indicate that *G. bulloides, "G." primordius*, and *G. altiaperturus* are surface dwellers (lowest $\delta^{18}O$ and highest $\delta^{13}C$), *P. bella* and *P. siakensis/mayeri* are thermocline dwellers, and *C. dissimilis*, *C. ciperoensis*, and *C. indianus* are sub-thermocline dwellers (highest $\delta^{18}O$ and lowest $\delta^{13}C$).

Our $\delta^{18}O$ and $\delta^{13}C$ data for *"D." venezuelana* morphotype 1 suggest that this taxon calcified in the lower thermocline in all four samples spanning the O/M boundary at Ceara Rise (Figure 3 I to IV), with no indication of calcification in the mixed layer, as observed in the equatorial Pacific and Gulf of Mexico (Poore and Matthews, 1984; Wade et al., 2007). Our inferred lower thermocline depth habitat for *"D." venezuelana* is consistent with the limited data previously available from O/M boundary sediments in the equatorial Atlantic (Biolzi, 1983; Pearson et al., 1997; Pearson and Wade, 2009). This observation prompts us to question whether the variation in inferred calcification depth of *"D." venezuelana* in the literature (Figure 2) is a geographical or temporal phenomenon. We note that studies of material pre-dating the mid-Oligocene assign a surface water habitat to *"D." venezuelana* (Poore and Matthews, 1984; Wade et al., 2007), whereas analyses of material of mid-Miocene or younger age report a deep-water calcification depth for *"D." venezuelana* (Barrera et al., 1985; Hodell and Vayavananda, 1993; Keller, 1985; Norris et al., 1993; Pearson et al., 2001; Pearson and Shackleton, 1995; Smart and Thomas, 2006). Taken together with our new results, this observation suggests that *"D." venezuelana* has changed its depth habitat over time. A habitat shift such as this has also been invoked to explain a mid-Oligocene (~27 Ma) increase in the $\delta^{18}O$ time series of *"D." venezuelana* in the absence of an associated shift in benthic $\delta^{18}O$ (Wade and Pälike, 2004). A study of O/M boundary

planktic foraminifera in the Indian Ocean reports a lowermost thermocline to sub-thermocline depth habitat for *"D." venezuelana* (Spezzaferri and Pearson, 2009), which in conjunction with previous studies and our new data suggests that the transition from a surface to a sub-thermocline habitat was complete shortly after the early Miocene. Changes in preferred calcification depth of planktic foraminifera are not uncommon on long (geological) timescales; taxa are reported to have shifted habitat both up (e.g. Coxall et al., 2000; Coxall et al., 2007) and down (e.g. Norris et al., 1993) the water column through time.

In our dataset, $\delta^{18}O$ and $\delta^{13}C$ fall within the same range for all three morphotypes of *"D." venezuelana* (Figure 3 I′ and IV′), implying the same (lower thermocline) depth habitat. This consistency is true for samples from both the upper Oligocene (I) and the lower Miocene (IV). The close similarity in inferred calcification depth for all three morphotypes strongly suggests that they need not be separated where large samples are required (e.g., to generate palaeoceanographic records of silicate weathering using Nd and Li isotope methods).

4.2. Geochemical changes with ontogeny

4.2.1 Late Oligocene (Sample I)

In our upper Oligocene sample there is tight grouping of $\delta^{18}O$ and Mg/Ca within each size fraction of *"D." venezuelana*, for all three morphotypes (Figure 4b and d). These data suggest that smaller *"D." venezuelana* calcify under the warmest conditions, higher in the water column, while intermediate to larger individuals calcify in slightly deeper, cooler waters.

The covariation in Mg/Ca and $\delta^{18}O$ within sample I implies that temperature is the dominant control on $\delta^{18}O_c$, given the strong temperature dependence of Mg/Ca in planktic foraminiferal calcite (Anand et al., 2003; Elderfield and Ganssen, 2000). The temperature of calcification can be estimated from Mg/Ca as follows, using the multispecies calibration of Anand et al. (2003),

$$Mg/Ca_{foram} = 0.38 \exp (0.090*T) \qquad (1)$$

where T is temperature (°C) and Mg/Ca_{foram} is the Mg/Ca of foraminiferal calcite, reported in mmol/mol. Using this equation we calculate calcification temperatures for *"D." venezuelana* in our upper Oligocene sample ranging from ~ 20 to ~ 22 ºC. It is important to note that, although Equation 1 is generally applicable to all modern planktic foraminifera species, the values of the constants are species specific (Anand et al., 2003). *"D." venezuelana* is an extinct taxa, so we cannot evaluate directly the extent to which these constants are appropriate. However, substituting the constants in Equation 1 with those determined for

Neogloboquadrina dutertrei, a modern thermocline-dwelling species, yields Mg/Ca temperatures that are only about 1 ºC warmer. A more important source of uncertainty in absolute temperatures is that Equation 1 assumes the Mg/Ca ratio of seawater of the Oligo-Miocene is the same as it is today, while numerous lines of evidence suggest that the Mg/Ca ratio of seawater has increased over the Cenozoic (Broecker and Yu, 2011; Coggon et al., 2010; Dickson, 2002; Hardie, 1996; Stanley and Hardie, 1998; Tyrrell and Zeebe, 2004; Wilkinson and Algeo, 1989). Assuming that seawater Mg/Ca was lower in the late Oligocene than today, failure to adjust for this factor yields artificially cool calcification temperatures. We evaluate this effect by adjusting the pre-exponent (*cf.* Lear et al., 2000) of the Anand et al., (2003) temperature equation as follows,

(2)

where Mg/Ca_{sw} is the Mg/Ca composition of modern seawater (~5.17 mol/mol) and $Mg/Ca_{sw\text{-}OM}$ is the estimated Mg/Ca composition of the ocean at O/M boundary time. Estimates of the secular shifts in oceanic Mg/Ca composition yield $Mg/Ca_{sw\text{-}OM}$ values ranging from 2 mol/mol (Coggon et al., 2010) to 4 mol/mol (Wilkinson and Algeo, 1989). Using this range of $Mg/Ca_{sw\text{-}OM}$ estimates in Equation 2, calcification temperatures of *"D." venezuelana* increase by 3 to 9 ºC compared to our original estimates, but the temperature offset between size fractions does not change.

The temperature of calcification can also be estimated from $\delta^{18}O$. We use the temperature calibration for the modern planktic foraminifera *Orbulina universa* (low light) from Bemis et al., (1998),

$$T\ (°C) = 16.5 - 4.8\ (\delta^{18}O_c - \delta^{18}O_{sw}) \qquad (3)$$

where $\delta^{18}O_{sw}$ for late Oligocene time is assumed to be -0.5‰ (Lear et al., 2004). Applying Equation 3 to our data, we obtain calcification temperatures for *"D." venezuelana* that are, on average, ~ 4°C lower than corresponding Mg/Ca-derived temperatures. $\delta^{18}O$ temperature calibrations are also species specific and the use of a temperature calibration for the modern planktic foraminifera *G. bulloides* (Bemis et al., 2000) yields $\delta^{18}O$ temperatures for *"D." venezuelana* that are a further 3°C lower but, once again, the range of temperatures calculated using $\delta^{18}O_c$ is not sensitive to choice of calibration. Discrepancy between $\delta^{18}O$- and Mg/Ca-derived estimates of absolute temperature is not unexpected in planktic foraminifera with a "frosty" taphonomy such as those from ODP Site 925, because of the apparently greater susceptibility of $\delta^{18}O_c$ to diagenetic alteration on the sea floor compared to Mg/Ca (Sexton et

al., 2006). Yet the range of calcification temperatures calculated for all morphotypes of *"D." venezuelana* (2-3°C) across all size fractions in our upper Oligocene sample is similar to that calculated from Mg/Ca.

The thermocline of the modern Ceara Rise exhibits negligible seasonal variation in depth and has a maximum temperature gradient of 1.3°C per 10 m increase in water depth (Levitus and Boyer, 1994). Our calculated 2 to 3°C range in calcification temperature, estimated using two independent temperature proxies, is very consistent with findings of previous studies (Nathan and Leckie, 2009; Wade et al., 2007) and suggests that *"D." venezuelana* migrates vertically downwards in the water column during its life cycle by up to 20 m. We conclude, therefore, that the anomalously low $\delta^{18}O$ value of *"D." venezuelana* recorded in the equatorial Pacific may at least in part result from, as suggested by Wade et al., (2007), the use of the smaller and restricted, 300-355 μm size fraction.

4.2.2 Early Miocene (Sample IV)

Our data show greater spread in $\delta^{18}O$ and Mg/Ca in the early Miocene (Figure 4a & c) than is the case for the late Oligocene, with no consistent pattern of change with test size. We consider two potential explanations to account for these observations; firstly, poorer sample preservation in the early Miocene, and secondly, instability of the tropical Atlantic thermocline in the early Miocene.

At low latitudes, in general, planktic $\delta^{18}O$ increases during post-depositional alteration because of the steep vertical oceanic temperature gradient, however Mg/Ca can either increase or decrease depending on the partition coefficients of Mg into biogenic vs. inorganic calcite (Sexton et al., 2006). We note four lines of evidence that suggest that our Oligocene versus Miocene results in test $\delta^{18}O$ and Mg/Ca are not attributable to the diagenetic histories of the samples analysed. (i) During our examination of ODP Site 925 material under the binocular light microscope we observed no discernable taphonomic offset between material of late Oligocene and early Miocene age. (ii) The preservation of *"D." venezuelana* in both samples can also be assessed by scanning electron microscope (SEM) analysis of test wall textures. Plate 3 shows that tests from both samples have been subject to recrystallisation, and can be considered to exhibit "frosty" taphonomy in the nomenclature of Sexton et al., (2006). Test architecture at the micron scale has been obscured by cemented overgrowths of inorganic calcite; however, the coarse cancellate wall structure is still visible in all of the tests examined. The degree of surface recrystallisation is shown to be similar in both samples. (iii) Cross sections through the test wall are shown in Plate 4. A distinctive layer, marking the original position of the primary organic membrane (POM), the site of initial calcification, is

still visible in all specimens. Post depositional precipitation of inorganic calcite inside tests has the potential to obscure primary shell chemistry. However, we find the extent to which this internal recrystallisation has taken place to be no more pronounced in our lower Miocene sample (Plate 4 IV a-e) than in our upper Oligocene sample (Plate 4 I a-e). (iv) Oligocene and Miocene age ODP cores from Ceara Rise exhibit changes in calcium carbonate content that are linked to inferred glacial-interglacial cycles. Glacial intervals, characterised by high benthic $\delta^{18}O$ (Pälike et al., 2006a; Zachos et al., 2001), coincide with peaks in magnetic susceptibility and low colour reflectance. These dark bands result from carbonate dissolution and contain poorer preserved microfossils (Shipboard Scientific Party, 1995a). Based on colour reflectance data, calibrated versus low-resolution weight percent calcium carbonate, we estimate the carbonate content of our upper Oligocene and lower Miocene samples to be, respectively, 61% and 63%; a feature that, along with our other observations, suggests preservation between samples is comparable.

We also consider the possibility that the different ontogenetic results that we obtain for $\delta^{18}O$ and Mg/Ca in our Oligocene versus Miocene samples are attributable to instability in the tropical Atlantic thermocline in the early Miocene. Global coupled climate models suggest that there were considerable changes in ocean circulation from the late Oligocene to the early Miocene, including a flow reversal through the Central American Seaway (CAS) that bathed the Caribbean Sea and western equatorial Atlantic in cooler, less saline Pacific waters (Bernsen and Dijkstra, 2010; von der Heydt and Dijkstra, 2005; von der Heydt and Dijkstra, 2006). In these simulations, the persistence of eastern equatorial winds maintains a westward flow of uppermost surface waters forcing the bulk of the newly induced eastern flow through the CAS to occur at depths of 100m (von der Heydt and Dijkstra, 2005; von der Heydt and Dijkstra, 2006). Input of Pacific waters, sourced from seasonal upwelling zones, is thought to have reduced the surface temperature of the tropical equatorial Atlantic by more than 1 °C (von der Heydt and Dijkstra, 2005). Given the depth of flow, upwelling source, and magnitude of cooling induced by the Pacific waters entering the Atlantic Ocean during the early Miocene it is reasonable to expect seasonal shifts in the thermocline at Ceara Rise that might act to help obscure systematic variations in $\delta^{18}O$ and Mg/Ca of *"D." venezuelana* with test size. Species inhabiting the tropics exhibit little seasonal variation in calcification rate (Kucera et al., 2007) allowing *"D." venezuelana*, with its high geochemical sensitivity to changes in vertical temperature regime, to capture such intra-annual temperature variation. High variability of stable isotope data in *"D." venezuelana,* relative to other planktic foraminifera, is also reported in mid-Miocene samples from the western equatorial Pacific, for which similar thermocline instability is invoked (Nathan and Leckie, 2009). If our

interpretation is correct, then the potentially implied changes in ocean circulation will have important implications for some silicate weathering proxies, particularly those with short ocean residence times, such as neodymium.

4.3. Symbiont palaeoecology

Steep carbon isotopic gradients with increasing planktic foraminiferal test size are generally associated with photosymbiont activity, specifically of dinoflagellates, whereas shallow gradients are more commonly associated with asymbiotic or chrysophyte symbiont-bearing species (Bornemann and Norris, 2007; D'Hondt et al., 1994; Elderfield et al., 2002; Pearson et al., 1993; Spero and Williams, 1988). To investigate the potential footprint of photosymbionts in our *"D." venezuelana* specimens, we compare our multiple size fraction $\delta^{13}C$ data in Figure 4e and f to similar data from known photosymbiont bearing and asymbiotic planktic foraminifera recovered from modern core-tops at two western equatorial Atlantic sites (Ravelo and Fairbanks, 1995). We normalise these core-top $\delta^{13}C$ data by matching the y-intercept of each line of best fit to that of our *"D." venezuelana* $\delta^{13}C$ results from sample I and sample IV. This exercise allows us to adjust for temporal changes in oceanic $\delta^{13}C$ (Figure 1) and thereby isolate the $\delta^{13}C$ gradient. Solid red lines in Figure 4e & f depict the steeper $\delta^{13}C$ gradients ($\Delta\delta^{13}C$/100 μm >0.2‰) of known photosymbiont bearing planktic foraminifera, whereas the dashed black lines show the more modest gradients ($\Delta\delta^{13}C$/100 μm <0.2‰) of living asymbiotic taxa. These data describe a continuum of gradients rather than two completely distinct populations presumably reflecting other influences on test $\delta^{13}C$ (e.g. physiological effects or symbiont type) that sometimes make the application of this approach to fossil taxa less than straightforward (e.g. Bornemann and Norris, 2007; Norris, 1998; Norris and Wilson, 1998).

The shallow $\delta^{13}C$ gradient that we document in the Miocene for sample I lies within the zone of known modern asymbiotic taxa while the data for sample IV fall on the dividing line between modern asymbiotic and dinoflagellate-bearing taxa. The only moderate enrichment of ^{13}C in larger *"D." venezuelana* specimens, along with its inferred lower thermocline depth habitat, implies that this species is asymbiotic (rather than hosting chrysophyte symbionts) similar to many Oligocene planktic foraminifera (Wade et al., 2008).

5. Conclusions and Implications

The planktic foraminifera species *"D." venezuelana* appears to have calcified within the lower thermocline during the late Oligocene and the early Miocene at Ceara Rise in the western equatorial Atlantic. This means that variations in the chemical composition of the

tests over this interval should reflect environmental changes in ocean chemistry, rather than changes in depth habitat. However, over longer time periods (tens of millions of years), *"D." venezuelana* appears to have shifted its depth of calcification from surface waters, to thermocline (during the late Oligocene to early Miocene), to sub-thermocline waters. This secular change from surface to deep-water depth habitat must be taken into consideration when interpreting long-term records. For example, Li/Ca ratios in planktic foraminifera may be, in part, regulated by the carbonate ion concentration [CO_3^{2-}] of seawater (Hall and Chan, 2004). [CO_3^{2-}] decreases with depth in the oceans, therefore a change in calcification depth of *"D." venezuelana* from the early Oligocene to late Miocene may act to amplify or dampen changes in the Li concentration of seawater.

Detailed analyses of $\delta^{18}O$, $\delta^{13}C$ and Mg/Ca in different size fractions, in conjunction with previous studies, reveal that, in the late Oligocene, *"D." venezuelana* shows ontogenetic variations in its depth habitat with younger specimens calcifying high in the water column followed by a descent to deeper calcification depths in the later stages of development. We therefore recommend the use of the large, >355 μm, size fraction for the purposes of generating geochemical time-series records (e.g. Nathan and Leckie, 2009). These ontogenetic changes are not evident in our early Miocene data, possibly indicating instability of the Miocene thermocline.

Finally, we have distinguished three morphotypes of *"D." venezuelana* in this study, which all appear to have the same palaeoecology. It remains important to separate these morphotypes from species that share morphologically similarities, such as *D. globosa* and *D. altispira,* that were lower mixed layer or upper thermocline dwellers, (e.g. Gasperi and Kennett, 1993; Hodell and Vayavananda, 1993; Pearson and Shackleton, 1995), yet our finding that different morphotypes of *"D." venezuelana* are palaeoecologically inseparable is good news for geochemical proxy techniques that rely on the availability of unusually large samples of mono-specific foraminiferal calcite.

6. List of species

Planktic foraminifera

Catapsydrax ciperoensis (Cushman and Bermúdez, 1937)

Catapsydrax dissimilis (Cushman and Bermúdez, 1937)

Catapsydrax indianus Spezzaferri and Pearson, 2009

436 *"Dentoglobigerina" venezuelana* (Hedberg, 1937); see Pearson and Wade (2009) for further
437 details.

438 *Globigerina bulloides* d'Orbigny, 1926

439 *Globigerinoides altiaperturus* Bolli, 1957

440 *"Globigerinoides" primordius* Blow and Banner, 1962

441 *Paragloborotalia bella* (Jenkins, 1967)

442 *Paragloborotalia siakensis/mayeri* (LeRoy, 1939/Cushman and Ellisor, 1939)

443 **Benthic foraminifera**

444 *Cibicidoides mundulus* (Brady, Parker, and Jones, 1888)

445 *Oridorsalis umbonatus* (Reuss, 1851)

446 **Table 1:** Sample details. ODP sample identification given as Leg, Site, Hole, Core and
447 Interval (cm). Magnetochron assignment is based on correlation to Site 1090. Ages are
448 estimated using the Site 926 age model (Pälike et al., 2006a).

Sample #	ODP sample identification	Site 925 depth (mbsf)	Equivalent site 926 depth (mcd)	Inferred magnetochron	Age (Ma)
IV	154-925A-20R-2W, 130–132 cm	470.60	439.83	Base C6Ar	21.0
III	154-925A-22R-4W, 10–12 cm	491.70	488.27	Top C6Cn.1n	22.6
II	154-925A-22R-7W, 30–32 cm	496.40	492.26	Middle C6Cn.1n	22.7
I	154-925A-24R-1W, 110–112 cm	507.40	530.54	Top C7Bn.2n	24.2

449

450

451

452

453

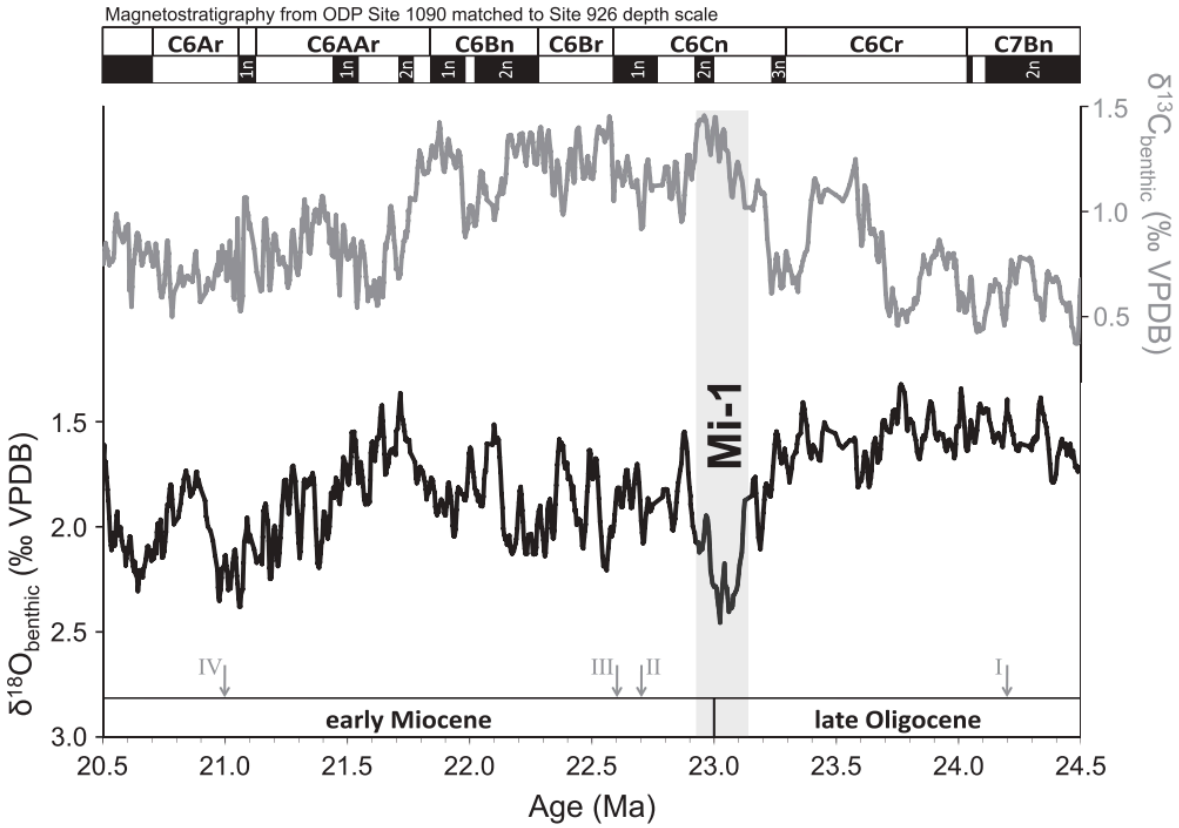

454

455 **Figure 1:** Benthic foraminiferal stable isotope records across the Oligocene-Miocene
456 boundary from ODP Site 926 (Pälike et al., 2006a). Solid black and grey lines show a 5-point
457 moving average of $\delta^{18}O$ and $\delta^{13}C$, respectively. Vertical grey bar highlights the Mi-1
458 excursion (Miller et al., 1991; Zachos et al., 2001). Grey arrows denote stratigraphic position
459 of samples investigated in this study (I-IV). Magnetostratigraphy from ODP Site 1090, South
460 Atlantic (Billups et al., 2002; Channell et al., 2003), correlated to Site 926 depth scale
461 (Liebrand et al., 2011), and matched through shipboard physical property data to Site 925
462 depth scale.

463

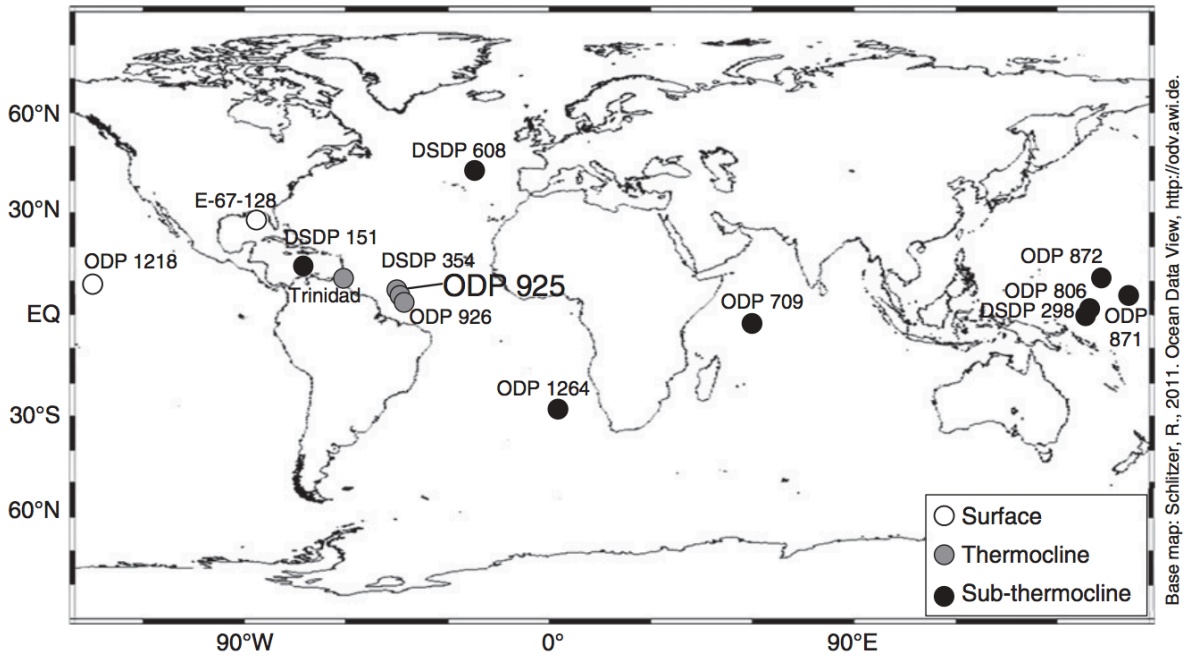

464

465 **Figure 2:** Location of ODP Site 925 in the equatorial Atlantic Ocean. Also shown are other
466 core sites for which the depth habitat (surface, thermocline or sub-thermocline) of *"D."*
467 *venezuelana* has been inferred from foraminiferal $\delta^{18}O$ and $\delta^{13}C$ (Biolzi, 1983; Hodell and
468 Vayavananda, 1993; Norris et al., 1993; Pearson et al., 2001; Pearson et al., 1997; Pearson
469 and Wade, 2009; Poore and Matthews, 1984; Smart and Thomas, 2006; Wade et al., 2007).

470

471

472

473

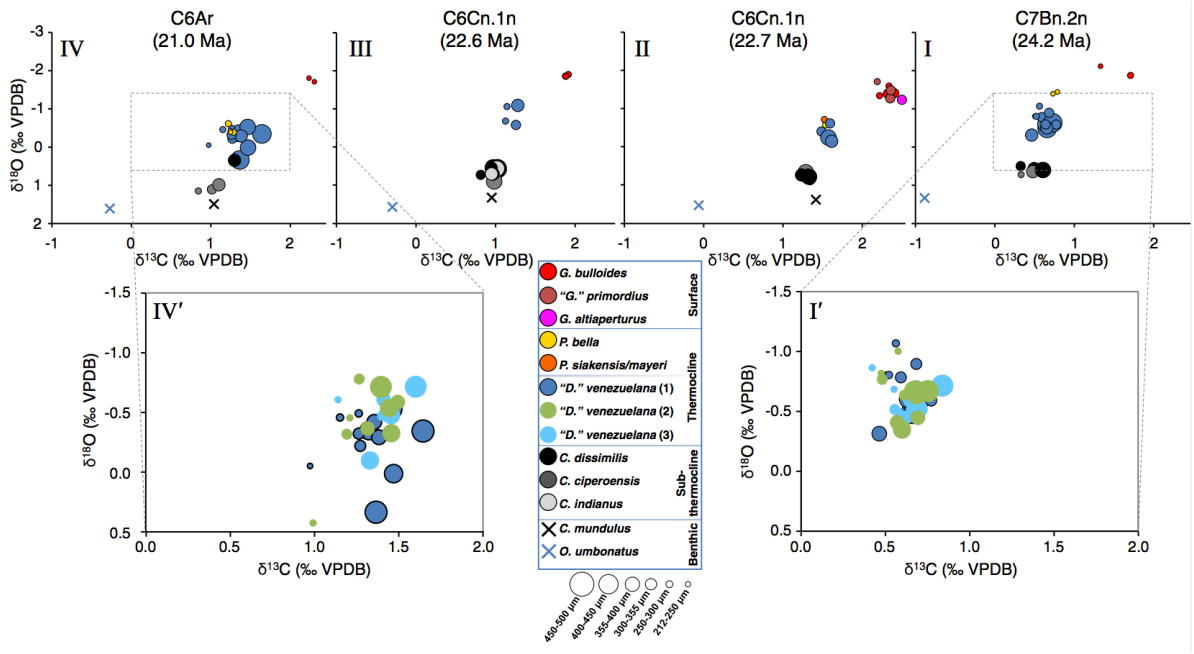

Figure 3: $\delta^{18}O$ and $\delta^{13}C$ in foraminiferal calcite recovered from ODP Site 925. The four samples (I – IV) span the O/M boundary. I′ and IV′ are enlarged sections of plots I and IV showing all *"D." venezuelana* morphotypes (morphotype 1 in dark blue, morphotype 2 in green and morphotype 3 in light blue). The colour and the size of the symbol schematically represent the species and the size fraction.

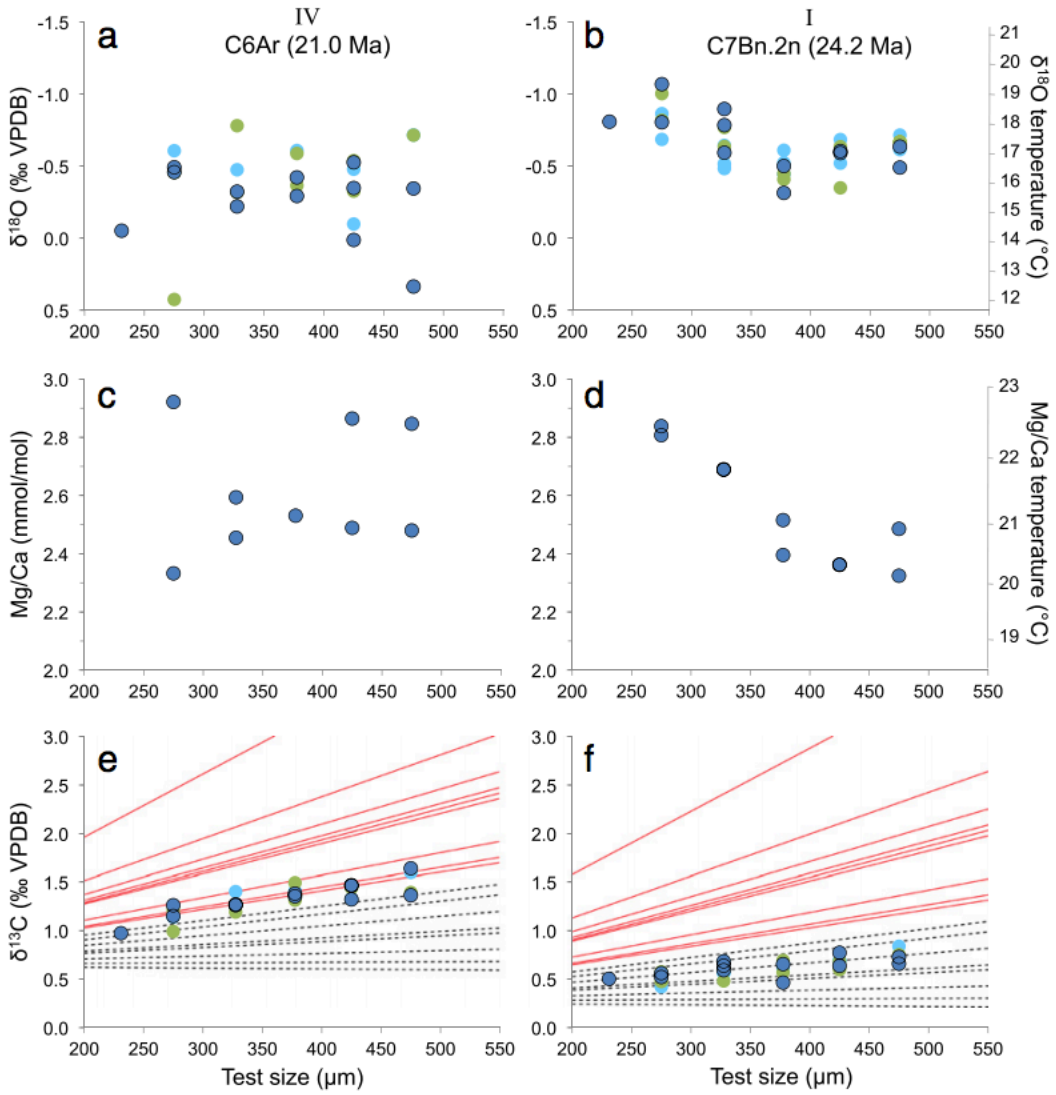

480

481 **Figure 4:** Changes in $\delta^{18}O$, $\delta^{13}C$ and Mg/Ca with test size of *"D." venezuelana*. Morphotype
482 1 (dark blue circles), 2 (green circles) and 3 (light blue circles). Mg/Ca temperature is derived
483 from an "all species" calibration (Equation 1; Anand et al., 2003). $\delta^{18}O$ temperature is
484 derived from Equation 3 (Bemis et al., 1998). Temperature scales apply only to Panels b and
485 d (sample I) and *not* to Panels a and c (see text for details). Lines in Panels e and f represent
486 the $\delta^{13}C$ gradients of modern symbiotic (solid red lines; *Globigerinoides ruber* (both pink and
487 white), *Globigerinoides aequilateralis*, *Globigerinoides sacculifer* (both with and without
488 sac), *Neogloboquadrina dutertrei*, *Globigerinoides conglobatus*, and *Orbulina universa*) and
489 asymbiotic plankic foraminifera (black dashed lines; *Globorotalia menardii*, *Globorotalia*
490 *truncatulinoides*, *Pulleniatina obliquiloculata*, *Globorotalia crassaformis*, *Globorotalia*
491 *tumida*) from two western equatorial Atlantic sites (Ravelo and Fairbanks, 1995).

492

493

494

495

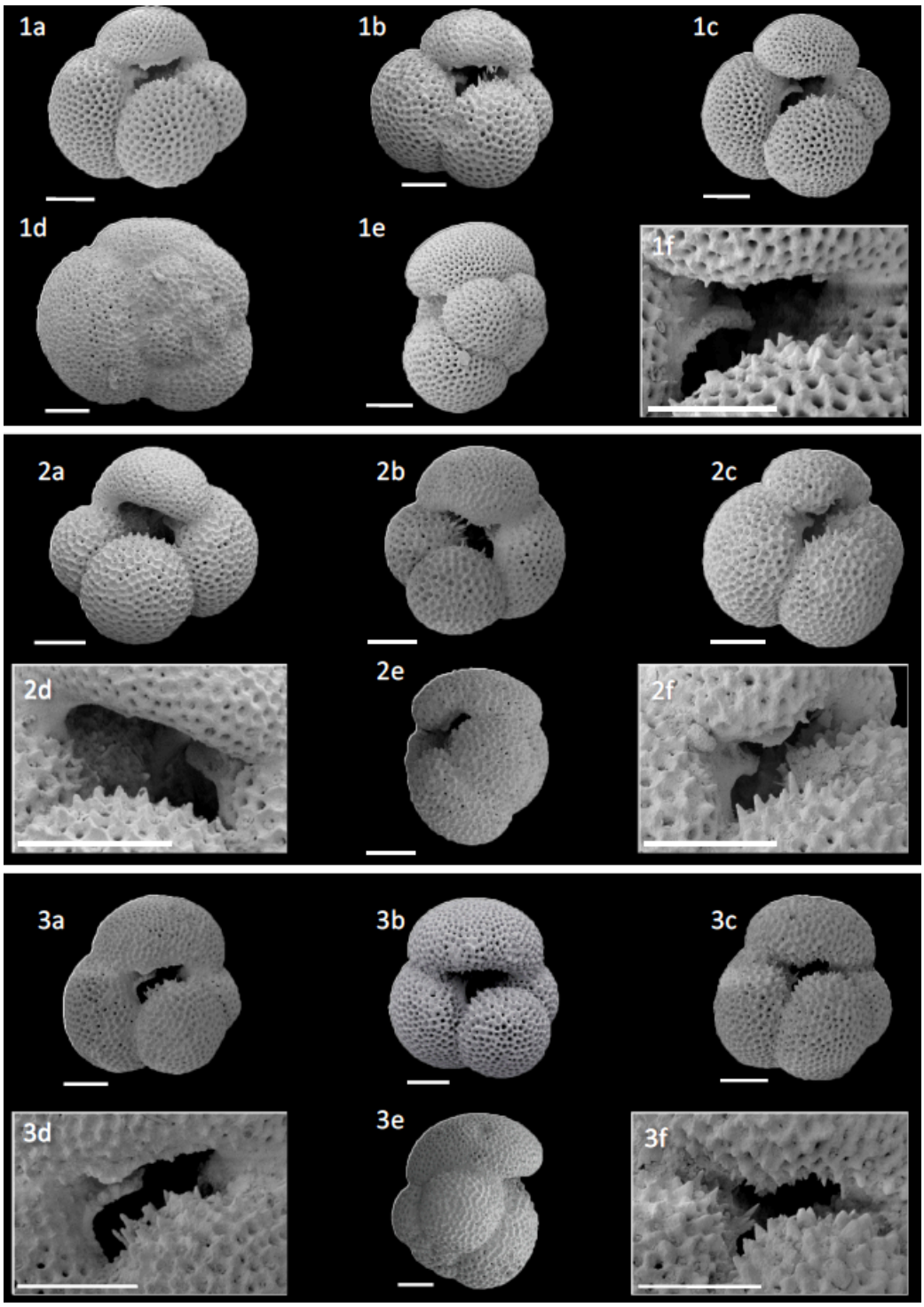

Plate 1: Scanning electron microscope images of *"Dentoglobigerina" venezuelana* morphotypes from ODP Site 925. All scale bars are 100 µm. **1(a-f).** *"D." venezuelana* morphotype 1, **1(a-c).** Umbilical views, 154-925A-24R-5W, 22-24 cm, **1d.** Spiral view, 154-925A-22R-7W, 30-32 cm, **1e.** Side view of specimen 1c, **1f.** Detailed wall texture and apertural view of specimen 1c. **2(a-f).** *"D." venezuelana* morphotype 2 (low arched aperture), **2(a-c).** Umbilical views, 154-925A-24R-5W, 22-24 cm, **2d.** Detailed wall texture and apertural view of specimen 2a, **2e.** Side view of specimen 2c, **2f.** Detailed wall texture and apertural view of specimen 2c, **3(a-f).** *"D." venezuelana* morphotype 3 (large final chamber), **3(a-c).** Umbilical views, 154-925A-24R-5W, 22-24 cm, **3d.** Detailed wall texture and apertural view of specimen 3a, **3e.** Side view, 154-925A-22R-7W, 30-32 cm, **3f.** Detailed wall texture and apertural view of specimen 3c.

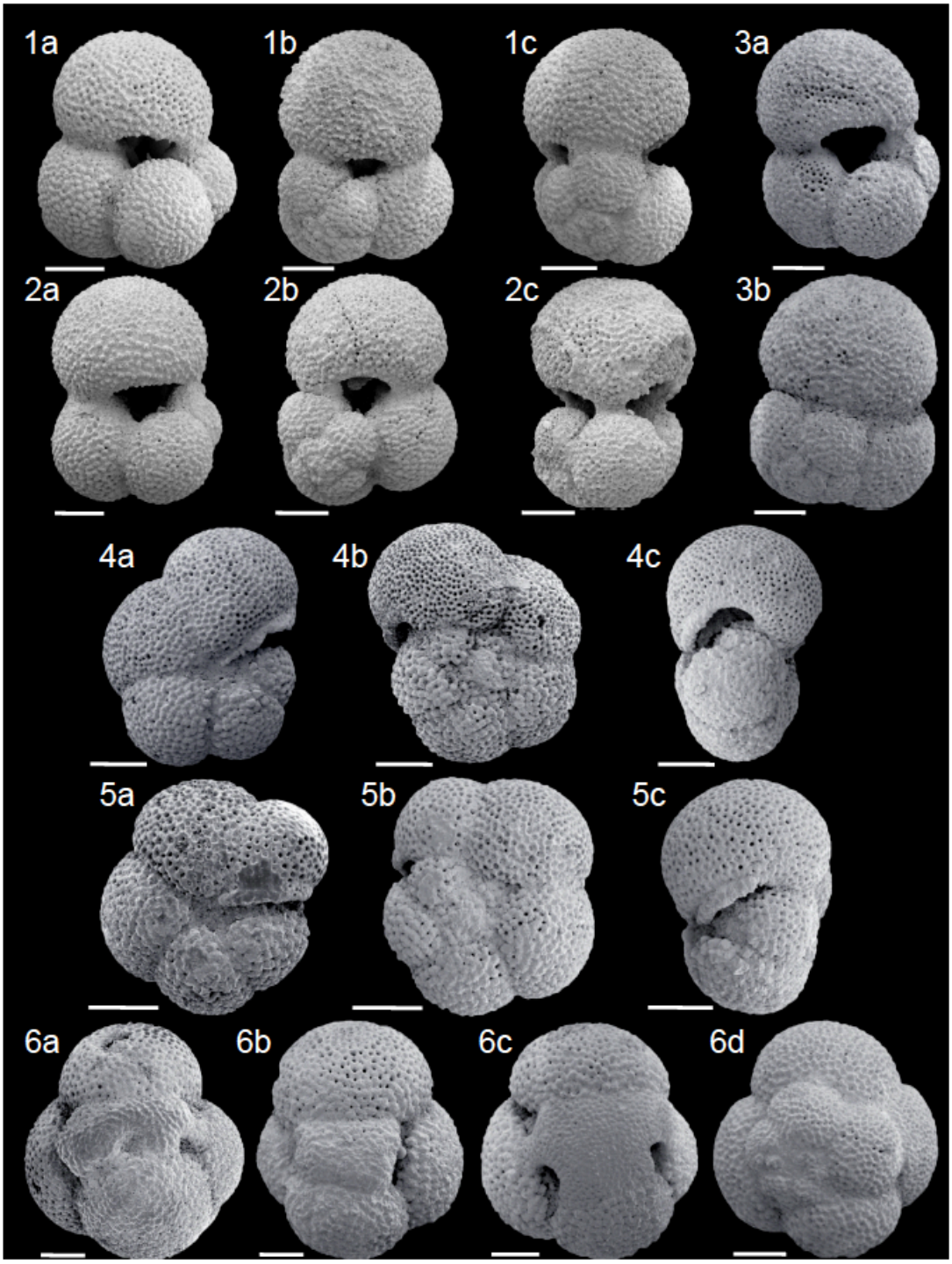

Plate 2: Scanning electron microscope images of Oligocene and Miocene planktic foraminifera from ODP Site 925 illustrating species concepts adopted in this study. All scale bars are 100 µm. **1(a-c).** *Globigerinoides primordius*, 154-925A-22R-7W, 30-32 cm, **1a.** Umbilical view, **1b.** Spiral view, **1c.** Side view, **2(a-c).** *Globigerinoides altiaperturus*, 154-925A-22R-7W, 30-32 cm, **2a.** Umbilical view, **2b.** Spiral view, **2c.** Side view, **3(a-b).** *Globigerina bulloides*, 154-925A-22R-7W, 30-32 cm, **3a.** Umbilical view, **3b.** Spiral view, **4(a-c).** *Paragloborotalia siakensis/mayeri*, 154-925A-22R-7W, 30-32 cm, **4a.** Umbilical view, **4b.** Spiral view, **4c.** Side view, **5(a-c).** *Paragloborotalia bella*, 154-925A-22R-7W, 30-32 cm, **5a.** Umbilical view, **5b.** Spiral view, **5c.** Side view, **6a.** *Catapsydrax indianus*, umbilical view, 154-925A-22R-4W, 10-12 cm, **6b.** *Catapsydrax dissimilis*, umbilical view, 154-925A-22R-7W, 30-32 cm, **6c.** *Catapsydrax ciperoensis*, umbilical view, 154-925A-22R-7W, 30-32 cm, **6d.** *Catapsydrax dissimilis*, spiral view, 154-925A-22R-7W, 30-32 cm.

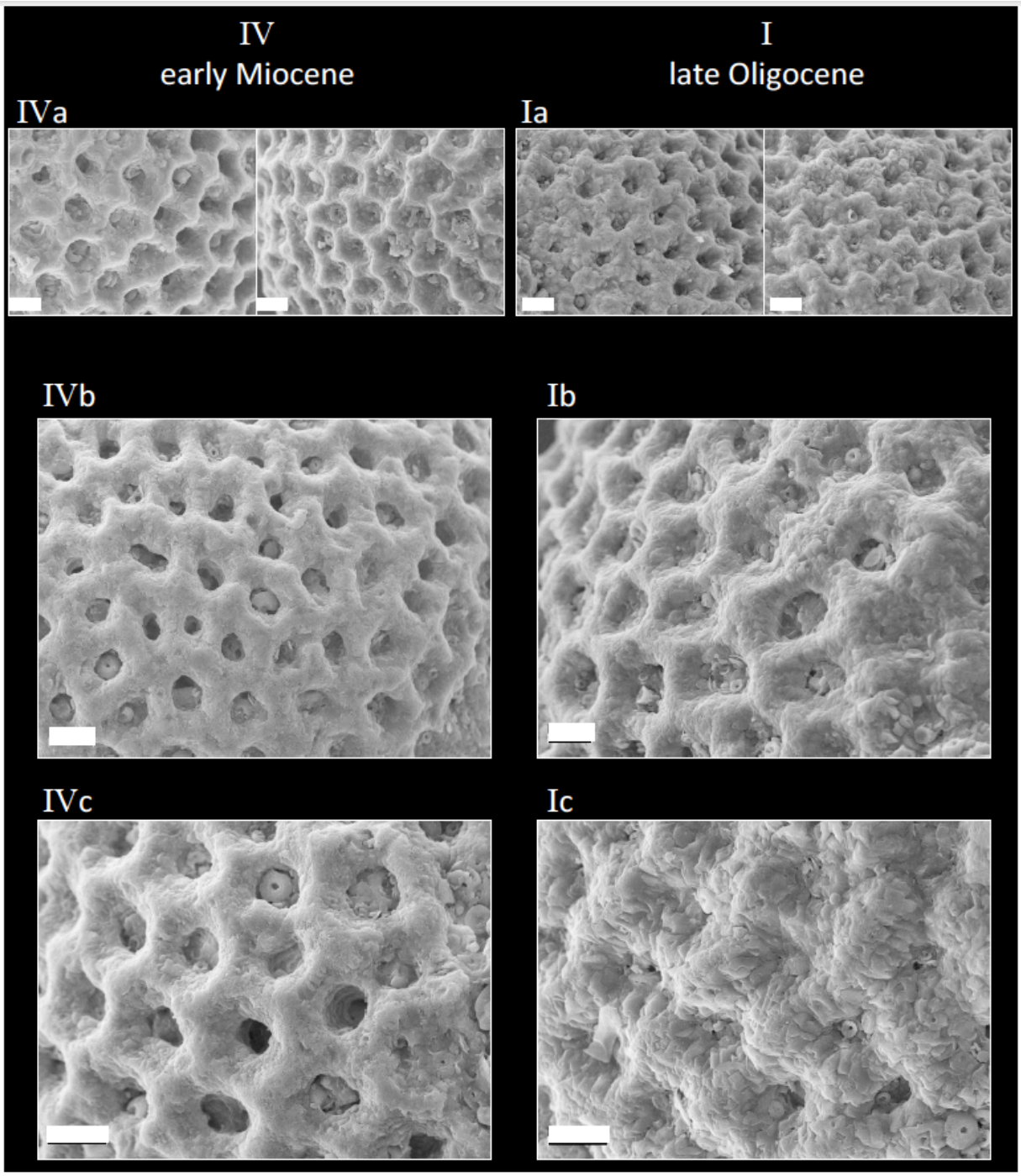

521

522 **Plate 3:** Scanning electron microscope images of *"D." venezuelana* morphotype 1 wall
523 textures from samples I (upper Oligocene) and IV (lower Miocene). All scale bars are 10 μm.

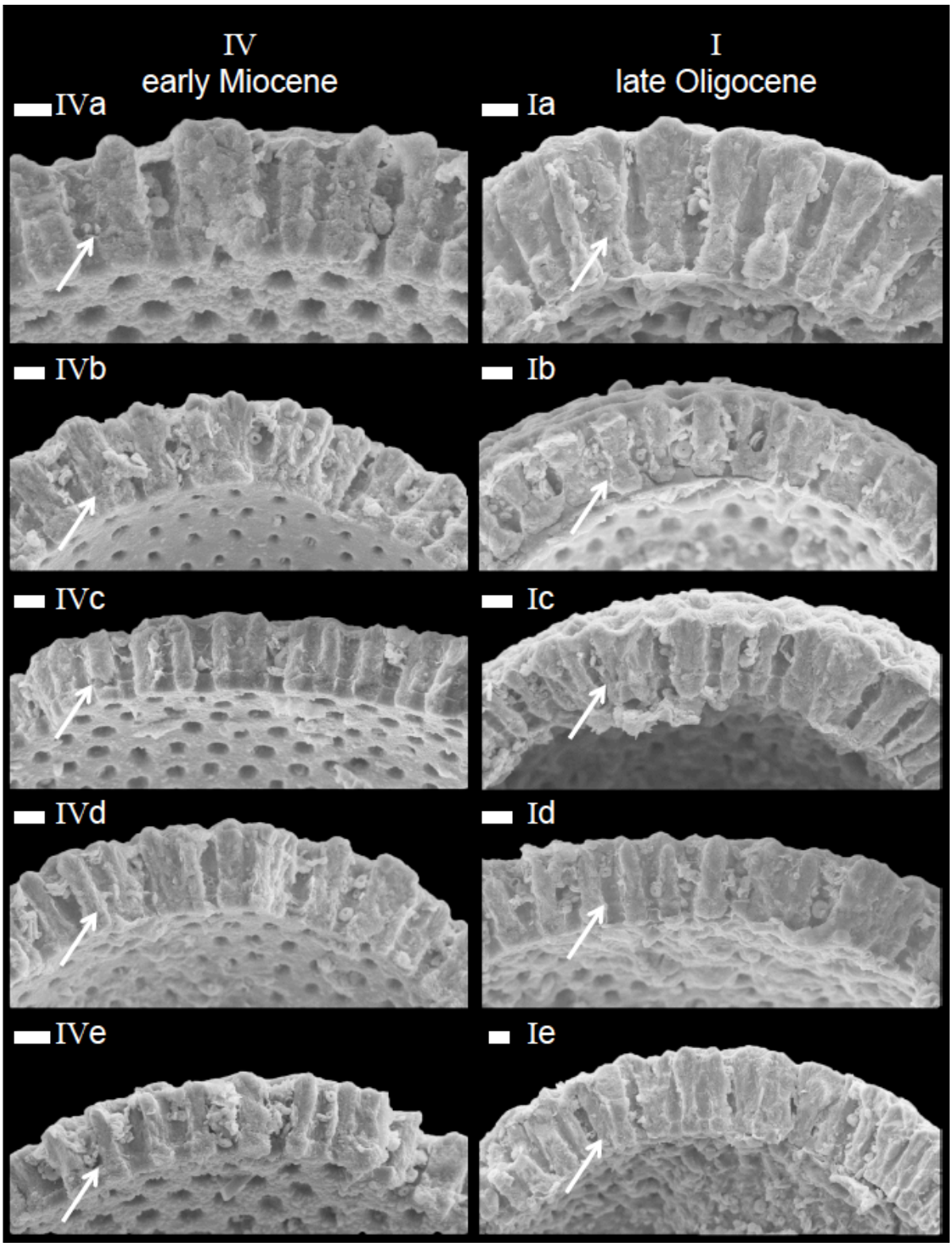

Plate 4: Scanning electron microscope images of *"D." venezuelana* morphotype 1 wall cross sections. All scale bars are 10 μm. White arrows show the original position of the primary organic membrane. **IV(a-e).** Test cross section images of *"D." venezuelana* from five different specimens in sample IV (lower Miocene). **I(a-e).** Test cross section images of *"D." venezuelana* from five different specimens in sample I (upper Oligocene).

Acknowledgements

This work used samples provided by the Ocean Drilling Program (ODP). The ODP (now IODP) is sponsored by the US National Science Foundation and participating countries under management of the Joint Oceanographic Institutions (JOI), Inc. We thank Walter Hale and staff at the Bremen Core Repository for their help obtaining core material and also Mike Bolshaw, Dave Spanner, Richard Pearce, and Darryl Green for help with laboratory work. We also thank Paul Pearson, Mark Leckie and Bridget Wade for their helpful and constructive reviews of this work. Financial support was provided by the UK Natural Environment Research Council, award # NE/D005108/1.

Footnotes

[1] S. Crowhurst, Department of Earth Sciences, University of Cambridge, Downing Street, Cambridge, CB2 3EQ, United Kingdom, sjc13@cam.ac.uk

References

Anand, P., Elderfield, H. and Conte, M.H., 2003. Calibration of Mg/Ca thermometry in planktonic foraminifera from a sediment trap time series. Paleoceanography, 18(2): 1050.

Barrera, E., Keller, G. and Savin, S.M., 1985. Evolution of the Miocene ocean in the eastern North Pacific as inferred from oxygen and carbon isotopic ratios of foraminifera. In: J.P. Kennett (Editor), The Miocene Ocean: Palaeoceanography and Biogeography. Geological Society of America Memoir 163, pp. 83-102.

Bemis, B.E., Spero, H.J., Bijma, J. and Lea, D.W., 1998. Reevaluation of the Oxygen Isotopic Composition of Planktonic Foraminifera: Experimental Results and Revised Paleotemperature Equations. Paleoceanography, 13(2): 150-160.

Bemis, B.E., Spero, H.J., Lea, D.W. and Bijma, J., 2000. Temperature influence on the carbon isotopic composition of Globigerina bulloides and Orbulina universa (planktonic foraminifera). Marine Micropaleontology, 38(3-4): 213-228.

Berner, R.A., 1991. A model for atmospheric CO_2 over Phanerozoic time. American Journal of Science, 291: 339-376.

Bernsen, E. and Dijkstra, H.A., 2010. Robustness of the Atlantic-Pacific flow reversal in the early miocene. Climate of the Past Discussions, 6(6): 2483-2516.

Billups, K., Channell, J.E.T. and Zachos, J., 2002. Late Oligocene to early Miocene geochronology and paleoceanography from the subantarctic South Atlantic. Paleoceanography, 17(1): 1004.

Biolzi, M., 1983. Stable isotopic study of Oligocene-Miocene sediments from DSDP Site 354, Equatorial Atlantic. Marine Micropaleontology, 8(2): 121-139.

Bolli, H.M. and Saunders, J.B., 1989. Oligocene to Holocene low latitude planktic foraminifera. In: H.M. Bolli, J.B. Saunders and K. Perch-Nielsen (Editors), Plankton stratigraphy. Cambridge University Press, pp. 155-262.

Bornemann, A. and Norris, R.D., 2007. Size-related stable isotope changes in Late Cretaceous planktic foraminifera: Implications for paleoecology and photosymbiosis. Marine Micropaleontology, 65(1-2): 32-42.

Boyle, E.A. and Keigwin, L.D., 1985. Comparison of Atlantic and Pacific paleochemical records for the last 215,000 years: changes in deep ocean circulation and chemical inventories. Earth and Planetary Science Letters, 76(1-2): 135-150.

Broecker, W. and Yu, J., 2011. What do we know about the evolution of Mg to Ca ratios in seawater? Paleoceanography, 26(3): PA3203.

Burton, K.W., Gannoun, A. and Parkinson, I.J., 2010. Climate driven glacial-interglacial variations in the osmium isotope composition of seawater recorded by planktic foraminifera. Earth and Planetary Science Letters, 295(1-2): 58-68.

Burton, K.W. and Vance, D., 2000. Glacial-interglacial variations in the neodymium isotope composition of seawater in the Bay of Bengal recorded by planktonic foraminifera. Earth and Planetary Science Letters, 176(3-4): 425-441.

Chaisson, W.P. and Leckie, M.R., 1993. High-resolution Neogene planktonic foraminiferal biostratigraphy of Site 806, Ontong Java Plateau (western equatorial Pacific). In: W.H. Berger, L.W. Kroenke, T.R. Janecek and W.V. Sliter (Editors), Proceedings of the Ocean Drilling Program, Scientific Results, pp. 130: 137-178.

Channell, J.E.T. et al., 2003. Eocene to Miocene magnetostratigraphy, biostratigraphy, and chemostratigraphy at ODP Site 1090 (sub-Antarctic South Atlantic). Geological Society of America Bulletin, 115(5): 607-623.

Coggon, R.M., Teagle, D.A.H., Smith-Duque, C.E., Alt, J.C. and Cooper, M.J., 2010. Reconstructing Past Seawater Mg/Ca and Sr/Ca from Mid-Ocean Ridge Flank Calcium Carbonate Veins. Science, 327(5969): 1114-1117.

595 Coxall, H.K., Pearson, P.N., Shackleton, N.J. and Hall, M.A., 2000. Hantkeninid depth
596 adaptation: An evolving life strategy in a changing ocean. Geology, 28(1): 87-90.
597 Coxall, H.K., Wilson, P.A., Pearson, P.N. and Sexton, P.F., 2007. Iterative evolution of
598 digitate planktonic foraminifera. Paleobiology, 33(4): 495-516.
599 D'Hondt, S., Zachos, J.C. and Schultz, G., 1994. Stable Isotopic Signals and Photosymbiosis
600 in Late Paleocene Planktic Foraminifera. Paleobiology, 20(3): 391-406.
601 Dickson, J.A.D., 2002. Fossil Echinoderms As Monitor of the Mg/Ca Ratio of Phanerozoic
602 Oceans. Science, 298(5596): 1222-1224.
603 Elderfield, H. and Ganssen, G., 2000. Past temperature and $\delta^{18}O$ of surface ocean waters
604 inferred from foraminiferal Mg/Ca ratios. Nature, 405(6785): 442-445.
605 Elderfield, H., Vautravers, M. and Cooper, M., 2002. The relationship between shell size and
606 Mg/Ca, Sr/Ca, $\delta^{18}O$, and $\delta^{13}C$ of species of planktonic foraminifera. Geochemistry
607 Geophysics Geosystems, 3(8): 1052.
608 Emiliani, C., 1955. Pleistocene temperatures. The Journal of Geology, 63: 40.
609 Frank, M., 2002. Radiogenic isotopes: Tracers of past ocean circulation and erosional input.
610 Rev. Geophys., 40(1): 1-38.
611 Gasperi, J.T. and Kennett, J.P., 1993. Vertical thermal structure evolution of Miocene surface
612 waters: Western equatorial Pacific DSDP Site 289. Marine Micropaleontology, 22(3):
613 235-254.
614 Greaves, M. et al., 2008. Interlaboratory comparison study of calibration standards for
615 foraminiferal Mg/Ca thermometry. Geochemistry Geophysics Geosystems, 9(8):
616 Q08010.
617 Green, D.R.H., Cooper, M.J., German, C.R. and Wilson, P.A., 2003. Optimization of an
618 inductively coupled plasma-optical emission spectrometry method for the rapid
619 determination of high-precision Mg/Ca and Sr/Ca in foraminiferal calcite.
620 Geochemistry Geophysics Geosystems, 4.
621 Hall, J.M. and Chan, L.H., 2004. Li/Ca in multiple species of benthic and planktonic
622 foraminifera: thermocline, latitudinal, and glacial-interglacial variation. Geochimica
623 et Cosmochimica Acta, 68(3): 529-545.
624 Hardie, L.A., 1996. Secular variation in seawater chemistry: An explanation for the coupled
625 secular variation in the mineralogies of marine limestones and potash evaporites over
626 the past 600 m.y. Geology, 24(3): 279-283.
627 Hathorne, E.C., 2004. The Trace Element and Lithium Isotope Composition of Planktonic
628 Foraminifera, Open University.
629 Hathorne, E.C. and James, R.H., 2006. Temporal record of lithium in seawater: A tracer for
630 silicate weathering? Earth and Planetary Science Letters, 246(3-4): 393-406.
631 Hedberg, H.D., 1937. Foraminifera of the middle Tertiary Carapita Formation of northeastern
632 Venezuela. Journal of Paleontology, 11(8): 661-697.
633 Hodell, D.A. and Vayavananda, A., 1993. Middle Miocene paleoceanography of the western
634 equatorial Pacific (DSDP site 289) and the evolution of Globorotalia (Fohsella).
635 Marine Micropaleontology, 22(4): 279-310.
636 Huh, Y., Chan, L.H. and Edmond, J.M., 2001. Lithium isotopes as a probe of weathering
637 processes: Orinoco River. Earth and Planetary Science Letters, 194(1-2): 189-199.
638 Jeandel, C., 1993. Concentration and isotopic composition of Nd in the South Atlantic Ocean.
639 Earth and Planetary Science Letters, 117(3-4): 581-591.
640 Keller, G., 1985. Depth stratification of planktonic foraminifers in the Miocene ocean. In:
641 J.P. Kennett (Editor), The Miocene Ocean: Palaeoceanography and Biogeography.
642 Geological Society of America Memoir 163, pp. 177−196.
643 Kennett, J.P. and Srinivasan, M.S., 1983. Neogene Planktonic Foraminifera: A Phylogenetic
644 Atlas. Hutchinson Ross.

645 Kisakürek, B., James, R.H. and Harris, N.B.W., 2005. Li and δ^7Li in Himalayan rivers:
646 Proxies for silicate weathering? Earth and Planetary Science Letters, 237(3-4): 387-
647 401.
648 Kroopnick, P.M., 1985. The distribution of ^{13}C of ΣCO_2 in the world oceans. Deep Sea
649 Research Part A. Oceanographic Research Papers, 32(1): 57-84.
650 Kucera, M., Claude, H.-M. and Anne De, V., 2007. Chapter Six Planktonic Foraminifera as
651 Tracers of Past Oceanic Environments, Developments in Marine Geology. Elsevier,
652 pp. 213-262.
653 Kump, L.R. et al., 1999. A weathering hypothesis for glaciation at high atmospheric pCO_2
654 during the Late Ordovician. Palaeogeography, Palaeoclimatology, Palaeoecology,
655 152(1-2): 173-187.
656 Lear, C.H., Elderfield, H. and Wilson, P.A., 2000. Cenozoic Deep-Sea Temperatures and
657 Global Ice Volumes from Mg/Ca in Benthic Foraminiferal Calcite. Science,
658 287(5451): 4.
659 Lear, C.H., Rosenthal, Y., Coxall, H.K. and Wilson, P.A., 2004. Late Eocene to early
660 Miocene ice sheet dynamics and the global carbon cycle. Paleoceanography,
661 19(PA4015): 1-11.
662 Leckie, R.M., Farnham, C. and Schmidt, M.G., 1993. Oligocene planktonic foraminifer
663 biostratigraphy of Hole 803D (Ontong Java Plateau) and Hole 628A (Little Bahama
664 Bank), and comparison with the southern high latitudes. In: W.H. Berger, L.W.
665 Kroenke, T.R. Janecek and W.V. Sliter (Editors), Proceedings of the Ocean Drilling
666 Program, Scientific Results, pp. 130: 113-136.
667 Levitus, S. and Boyer, T.P., 1994. World Ocean Atlas 1994 Volume 4: Temperature, 4.
668 Li, Q., McGowran, B. and Brunner C. A., 2002. Neogene Planktonic Foraminiferal
669 Biostratigraphy of Sites 1126, 1128, 1130, 1132, and 1134, ODP Leg 182, Great
670 Australian Bight. In: A.C. Hine, D.A. Feary and Malone M. J. (Editors), Proceedings
671 of the Ocean Drilling Program, Scientific Results.
672 Liebrand, D. et al., 2011. Antarctic ice sheet and oceanographic response to eccentricity
673 forcing during the early Miocene. Climate of the Past, 7(3): 869-880.
674 Miller, K.G., Wright, J.D. and Fairbanks, R.G., 1991. Unlocking the Ice House: Oligocene-
675 Miocene Oxygen Isotopes, Eustasy, and Margin Erosion. Journal of Geophysical
676 Research, 96(B4): 6829–6848.
677 Nathan, S.A. and Leckie, R.M., 2009. Early history of the Western Pacific Warm Pool during
678 the middle to late Miocene (~ 13.2–5.8 Ma): Role of sea-level change and
679 implications for equatorial circulation. Palaeogeography, Palaeoclimatology,
680 Palaeoecology, 274(3-4): 140-159.
681 Norris, R.D., 1998. Recognition and macroevolutionary significance of photosymbiosis in
682 molluscs, corals, and foraminifera. In: W.L. Manger and L.K. Meeks (Editors),
683 Isotope Paleobiology and Paleoecology. Paleontological Society Papers, 4, pp. 68–
684 100.
685 Norris, R.D., Corfield, R.M. and Cartlidge, J.E., 1993. Evolution of depth ecology in the
686 planktic foraminifera lineage Globorotalia (Fohsella). Geology, 21(11): 975-978.
687 Norris, R.D. and Wilson, P.A., 1998. Low-latitude sea-surface temperatures for the mid-
688 Cretaceous and the evolution of planktic foraminifera. Geology, 26(9): 823-826.
689 Olsson, R.K., Hemleben, C. and Pearson, P.N., 2006. Taxonomy, biostratigraphy and
690 phylogeny of Eocene *Dentoglobigerina*. In: P.N. Pearson, R.K. Olsson, B.T. Huber,
691 C. Hemleben and W.A. Berggren (Editors), Atlas of Eocene Planktonic Foraminifera.
692 Cushman Foundation Special Publication, 41, pp. 401-412.
693 Pälike, H., Frazier, J. and Zachos, J.C., 2006a. Extended orbitally forced palaeoclimatic
694 records from the equatorial Atlantic Ceara Rise. Quaternary Science Reviews, 25(23-
695 24): 3138-3149.

Pälike, H. et al., 2006b. The Heartbeat of the Oligocene Climate System. Science, 314(5807): 1894-1898.

Paul, H.A., Zachos, J.C., Flower, B.P. and Tripati, A., 2000. Orbitally induced climate and geochemical variability across the Oligocene/Miocene boundary. Paleoceanography, 15(5): 471.

Pearson, P.N. and Chaisson, W.P., 1997. Late Paleocene to middle Miocene planktonic foraminifer biostratigraphy of the Ceara Rise. In: N.J. Shackleton, W.B. Curry, C. Richter and T.J. Bralower (Editors), Proceedings of the Ocean Drilling Program, Scientific Results, pp. 154: 33-68.

Pearson, P.N., Norris, R.D. and Empson, A.J., 2001. Mutabella mirabilis Gen et Sp. Nov., a Miocene microperforate planktonic foraminifer with an extreme level of intraspecific variability. Journal of Foraminiferal Research, 31(2): 120-132.

Pearson, P.N. and Shackleton, N.J., 1995. Neogene Multispecies Planktonic Foraminifer Stable Isotope Record, Site 871, Limalok Guyot. In: J.A. Haggerty, I. Premoli Silva, F. Rack and M.K. McNutt (Editors), Proceedings of the Ocean Drilling Program, Scientific Results, pp. 144: 401-410.

Pearson, P.N., Shackleton, N.J. and Hall, M.A., 1993. Stable isotope paleoecology of middle Eocene planktonic foraminifera and multi-species isotope stratigraphy, DSDP Site 523, South Atlantic. Journal of Foraminiferal Research, 23(2): 123-140.

Pearson, P.N., Shackleton, N.J., Weedon, G.P. and Hall, M.A., 1997. Multispecies planktonic foraminifera stable isotope stratigraphy through Oligocene/Miocene boundary climatic cycles, Site 926. In: N.J. Shackleton, Curry, W.B., Richter, C., and Bralower, T.J. (Editor), Proceedings of the Ocean Drilling Program, Scientific Results, pp. 154: 441-449.

Pearson, P.N. and Wade, B.S., 2009. Taxonomy and stable isotope paleoecology of well-preserved planktonic foraminifera from the uppermost Oligocene of Trinidad. Journal of Foraminiferal Research, 39(3): 191-217.

Poore, R.Z. and Matthews, R.K., 1984. Oxygen isotope ranking of late Eocene and Oligocene planktonic foraminifers: Implications for Oligocene sea-surface temperatures and global ice-volume. Marine Micropaleontology, 9(2): 111-134.

Rathburn, A.E. and Corliss, B.H., 1994. The Ecology of Living (Stained) Deep-Sea Benthic Foraminifera from the Sulu Sea. Paleoceanography, 9(1): 87-150.

Ravelo, A.C. and Fairbanks, R.G., 1995. Carbon isotopic fractionation in multiple species of planktonic foraminifera from core-tops in the tropical Atlantic. Journal of Foraminiferal Research, 25(1): 53-74.

Ravizza, G. and Peucker-Ehrenbrink, B., 2003. The marine $^{187}Os/^{188}Os$ record of the Eocene-Oligocene transition: the interplay of weathering and glaciation. Earth and Planetary Science Letters, 210(1-2): 151-165.

Raymo, M.E. and Ruddiman, W.F., 1992. Tectonic forcing of late Cenozoic climate. Nature, 359(6391): 117-122.

Rosenthal, Y., Boyle, E.A. and Labeyrie, L., 1997. Last Glacial Maximum Paleochemistry and Deepwater Circulation in the Southern Ocean: Evidence From Foraminiferal Cadmium. Paleoceanography, 12(6): 787-796.

Rosenthal, Y., Field, M.P. and Sherrell, R.M., 1999. Precise determination of element/calcium ratios in calcareous samples using sector field inductively coupled plasma mass spectrometry. Analytical Chemistry, 71(15): 3248-3253.

Sexton, P.F., Wilson, P.A. and Pearson, P.N., 2006. Microstructural and geochemical perspectives on planktic foraminiferal preservation: "Glassy" versus "Frosty". Geochemistry Geophysics Geosystems, 7(12): Q12P19.

Shipboard Scientific Party, 1995a. Site 925. In: W.B. Curry, N.J. Shackleton, C. Richter and et al. (Editors), Proceedings of the Ocean Drilling Program. Initial Reports. College Station, TX (Ocean Drilling Program), pp. 154: 55-152.

748 Shipboard Scientific Party, 1995b. Site 926. In: W.B. Curry, N.J. Shackleton, C. Richter and
749 et al. (Editors), Proceedings of the Ocean Drilling Program. Initial Reports. College
750 Station, TX (Ocean Drilling Program), pp. 154: 153-232.
751 Smart, C.W. and Thomas, E., 2006. The enigma of early Miocene biserial planktic
752 foraminifera. Geology, 34(12): 1041-1044.
753 Spero, H.J. and Williams, D.F., 1988. Extracting environmental information from planktonic
754 foraminiferal $\delta^{13}C$ data. Nature, 335(6192): 717-719.
755 Spero, H.J. and Williams, D.F., 1989. Opening the Carbon Isotope "Vital Effect" Black Box
756 1. Seasonal Temperatures in the Euphotic Zone. Paleoceanography, 4(6): 593-601.
757 Spezzaferri, S., 1994. Planktonic foraminiferal biostratigraphy and taxonomy of the
758 Oligocene and lower Miocene in the oceanic record. An overview. Palaeontographia
759 Italica, 81: 188.
760 Spezzaferri, S. and Pearson, P.N., 2009. Distribution and Ecology of *Catapsydrax indianus*,
761 A New Planktonic Foraminifer Index Species for the Late Oligocene–Early Miocene.
762 Journal of Foraminiferal Research, 39(2): 112-119.
763 Stainforth, R.M., Lamb, J.L., Luterbacher, H., Beard, J.H. and Jeffords, R.M., 1975.
764 Cenozoic Planktonic Foraminiferal Zonation and Characteristics of Index Forms
765 (Appendix), Article 62. Univ. Kansas Paleontol. Contrib.
766 Stanley, S.M. and Hardie, L.A., 1998. Secular oscillations in the carbonate mineralogy of
767 reef-building and sediment-producing organisms driven by tectonically forced shifts
768 in seawater chemistry. Palaeogeography, Palaeoclimatology, Palaeoecology, 144(1-
769 2): 3-19.
770 Tyrrell, T. and Zeebe, R.E., 2004. History of carbonate ion concentration over the last 100
771 million years. Geochimica et Cosmochimica Acta, 68(17): 3521-3530.
772 Vance, D. and Burton, K., 1999. Neodymium isotopes in planktonic foraminifera: a record of
773 the response of continental weathering and ocean circulation rates to climate change.
774 Earth and Planetary Science Letters, 173(4): 365-379.
775 Vance, D., Teagle, D.A.H. and Foster, G.L., 2009. Variable Quaternary chemical weathering
776 fluxes and imbalances in marine geochemical budgets. Nature, 458(7237): 493-496.
777 von der Heydt, A. and Dijkstra, H.A., 2005. Flow reorganizations in the Panama Seaway: A
778 cause for the demise of Miocene corals? Geophys. Res. Lett., 32(2): L02609.
779 von der Heydt, A. and Dijkstra, H.A., 2006. Effect of ocean gateways on the global ocean
780 circulation in the late Oligocene and early Miocene. Paleoceanography, 21(1):
781 PA1011.
782 Wade, B., Al-Sabouni, N., Hemleben, C. and Kroon, D., 2008. Symbiont bleaching in fossil
783 planktonic foraminifera. Evolutionary Ecology, 22(2): 253-265.
784 Wade, B.S., Berggren, W.A. and Olsson, R.K., 2007. The biostratigraphy and paleobiology
785 of Oligocene planktonic foraminifera from the equatorial Pacific Ocean (ODP Site
786 1218). Marine Micropaleontology, 62(3): 167-179.
787 Wade, B.S. and Pälike, H., 2004. Oligocene climate dynamics. Paleoceanography, 19(4):
788 PA4019.
789 Walker, J.C.G., Hays, P.B. and Kasting, J.F., 1981. A negative feedback mechanism for the
790 long-term stabilization of the Earth's surface temperature. Journal of Geophysical
791 Research, 86(C10): 9776-9782.
792 Weedon, G.P., Shackleton, N.J. and Pearson, P.N., 1997. The Oligocene time scale and
793 cyclostratigraphy on the Ceara Rise, western equatorial Atlantic. In: N.J. Shackleton,
794 Curry, W.B., Richter, C., and Bralower, T.J. (Editor), Proceedings of the Ocean
795 Drilling Program, Scientific Results, pp. 154: 101-114.
796 Wilkinson, B.H. and Algeo, T.J., 1989. Sedimentary carbonate record of calcium-magnesium
797 cycling. American Journal of Science, 289(10): 1158-1194.

798 Zachos, J.C., Shackleton, N.J., Revenaugh, J.S., Palike, H. and Flower, B.P., 2001. Climate
799 response to orbital forcing across the Oligocene-Miocene boundary. Science,
800 292(5515): 274-278.
801
802
803